Physics Journal
Vol. 1, No. 1, 2015, pp. 1-9
http://www.aiscience.org/journal/pj

Two and Three Dimensional Investigation of Bubble Rising in High Density Ratio

Elham Sattari[1], Mojtaba Aghajani Delavar[1, *], Ehsan Fattahi[2], Korosh Sedighi[1]

[1]Department of Mechanical Engineering, Babol Noushirvani University of Technology, Babol, Iran
[2]Department of Numerical Mathematics, Technical University of Munich, Munich, Germany

Abstract

In present paper three-dimensional isothermal Lattice Boltzmann Method have been used to simulate the motion of bubble. The above model is unified with another two dimensional non-isothermal model in order to reduce computational cost. Firstly, it is ensured that the surface tension effect and Laplace law are properly implemented. Secondly, effect of governing dimensionless numbers on terminal Reynolds number and terminal shape of bubble are investigated in 3D and 2D simulations. Different flow patterns in various dimensionless numbers are obtained and by changing the dimensionless number, terminal change of bubble's shape are seen. The error of 2D solution is calculated. The results show that with increasing terminal Reynolds number increase the difference between 2D and 3D solutions and in high Reynolds number, 2D simulation for this phenomenon is not acceptable.

Keywords

Two Phase Flow, Lattice Boltzmann Method, Free Energy Approach

Received: May 3, 2015 / Accepted: May 21, 2015 / Published online: June 26, 2015

1. Introduction

In scientific point, many phenomena in daily life are two-phase or multiphase, for example, the raindrops motion; dust particles motion in the air or the wave motion on the sea surface and its failure modes are examples of two-phase issues occurs in nature. Two-phase fluid with many applications uses in industrial issues, for example, use in boilers. In boilers, combination of water and vapour as a two-phase fluid has an important role in boilers design.

In addition, two-phase fluid with main application is used in nuclear reactor design. As well as designing advanced tools like rocket engines, water purifiers and blood pumping machines need detailed knowledge in dynamic of multi-phase flow.

Checking the bubble motion in fluids is used in many applications such as petroleum and chemical industries and it is because of the mixture of gas and liquid broadly in these industries. The physical mechanism of two-phase flow is very complex. Thus, clear perception of two-phase flow mechanisms is not available. The numerical investigation in two-phase flows is significant due to disability of experimental investigations to access to the physical parameters in the bubble and droplet. Thus, numerical investigation is preferable for this phenomenon.

The lattice Boltzmann method is almost new numerical techniques based on kinetic theory, which is used for investigation of fluid flows. In Comparison with the traditional CFD, LBM has some advantages such as easy process, simple and efficient implementation for parallel computation, simple and strong handling of complex geometries, etc. There are various versions, which provided for two-phase flows using Lattice Boltzmann method.

* Corresponding author
E-mail address: m.a.delavar@nit.ac.ir (M. A. Delavar)

Gunstensen et al. [1] presented a multi component model based on two dimensional lattice-gas hydrodynamics. In their model two-particle distribution functions, red and blue, were introduced for studying two different fluids. Shan and Chen [2] offered a method for multicomponent and multiphase flows with regard microscopic interaction. Swift et al. [3] proposed a model for multiphase and multicomponent flows by using free energy approach. The main advantage of this model is the ability to include multi component and non-ideal thermodynamics of fluid in isothermal. It is worth mentioning that, in the all listed LBM two-phase models, the density ratio is intended less than 10, while in fact density ratio is more than 10 at most of the liquid-gas systems. Main problem in numerical solution of two-phase flow with large density ratio is numerical instability in interface. Inamuro et al. [4] offered a new model based on free energy approach for two-phase flow with high density ratio and investigated motion of a single bubble and many bubbles under buoyancy force in three dimensions(3D) simulation. Inamuro et al. [5] used their method to study rising of two droplets and their coalescence in a vertical and horizontal rectangular channel. In another study, Inamuro et al. [6] employed this model to simulate coalescence of two droplets with equal diameter with initial velocity in 3D and also of two droplets with unequal diameter in 3D [7] . Inamuro [8]carried out simulation of a set of bubbles in a branch channel, this geometry was utilized as a cooling system in air conditioning system. Yan and Zu [9] simulated horizontal movement of two bubbles with initial velocity in 3D channel.

Yoshino and Mizutani [10] studied contact angel by adding wettability condition to Inamuro [4] method. Yan and Zu [11] investigated the final shape of droplet on surface in different wettability and also they studied the final shape of droplet on partial wetting surface in 3D. In [12] Yan and Zu studied rising two bubbles, their coalescence and shape of droplet on partial wetting surface. Later on making some changes on the original model was used by Tanaka [13, 14] for two dimensional and reactive flows. Tanaka et al. [13] simulated dynamic treatment of droplet on solid surface. Moreover, they used this model for investigation of boiling process [14] . In addition to Inamuro [4] , Lee and others have presented their proposed method in two-phase fluid flows with high density difference [15-18] .

Inamuro model [4] is a 3D model so has high computational cost, Tanaka [14] added derivative of pressure tensor term to Inamuro [4] model for simulation of boiling in two dimensions and it increases computational cost in two dimensions. The difference between the presented model and former one [14] , which derived from Inamuro's model [4], is this model can simulate two-phase phenomenon with density ratio about 1000, while in former study [14] density ratio is about 50.

In this paper for the first time is used Inamuro's model in large density ratio about 1000 in two dimensions. First in this paper, by applying this model to ensure the proper functioning of the effect of surface tension in high density ratio about 1000. For this purpose, two tests have been conducted: the first test was related to a two dimensional square bubble, placed in a liquid. In the second test, two circular bubbles have been placed side by side and their approach was modelled. After that the Laplace law has been checked, and then the effect of dimensionless numbers for a bubble rising by buoyancy force have been investigated both 3D and 2D. The results of two-dimensional and three-dimensional solution were compared.

2. Methodology

In the present paper, the method introduced by Inamuro [4] is employed. Two distribution functions are used, f_i is used to calculate order parameter which distinguish two phases, and g_i is implemented to calculate a predicted velocity of the two-phase fluid without a pressure gradient. The particle distribution functions $f_i(x,t)$ and $g_i(x,t)$ with velocity c_i and at point x and time t is calculated by following equations [4]:

$$f_i(x+c_i\Delta x, t+\Delta t) = f_i^c(x,t) \tag{1}$$

$$g_i(x+c_i\Delta x, t+\Delta t) = g_i^c(x,t) \tag{2}$$

f_i^c and g_i^c are equilibrium distribution functions, Δx is spacing of square lattice, Δt is time step in the scale of LBM during which particles move in lattice spacing. Order parameter ϕ distinguishes two phases and the predicted velocity u^* of the multi-component fluid is defined according to two particle velocity distribution function as :

$$\phi = \sum_{i=0}^{8} f_i, \tag{3}$$

$$u^* = \sum_{i=0}^{8} g_i c_i \tag{4}$$

Equilibrium distribution functions in Eqs. (1) and (2) are described as:

$$f_i^c = H_i\phi + F_i\left[p_0 - k_f\phi\frac{\partial^2\phi}{\partial x_\alpha}\right] + 3E_i\phi c_{i\alpha}u_\alpha + E_i k_f G_{\alpha\beta}(\phi)c_{i\alpha}c_{i\beta} \tag{5}$$

$$
\begin{aligned}
g_i^c &= E_i\left[1+3c_{i\alpha}u_\alpha-\frac{3}{2}u_\alpha u_\alpha+\frac{9}{2}c_{i\alpha}c_{i\beta}u_\alpha u_\beta\right]\\
&+E_i+\frac{3}{4}\Delta x\left(\frac{\partial u_\beta}{\partial x_\alpha}+\frac{\partial u_\alpha}{\partial u_\beta}\right)c_{i\alpha}c_{i\beta}-3E_i c_{i\gamma}\left(1-\frac{\rho_G}{\rho}\right)g\Delta x\\
&+E_i\left[3c_{i\alpha}\frac{\Delta x}{\rho}\frac{\partial}{\partial x_\beta}\left\{\frac{\partial u_\beta}{\partial x_\alpha}+\frac{\partial u_\alpha}{\partial x_\beta}\right\}\right]\\
&+E_i\frac{k_g}{\rho}G_{\alpha\beta}(\rho)c_{i\alpha}c_{i\beta}-\frac{1}{2}F_i\frac{k_g}{\rho}\left(\frac{\partial\rho}{\partial x_\alpha}\right)^2
\end{aligned}
\tag{6}
$$

where g is the gravitational acceleration, and ρ , ρ_L , μ are density, density of liquid and viscosity of liquid, respectively, which are determined regarding to density ratio (e.g. if $\rho_L/\rho_G=50$ then $\rho_L=50$, $\rho_G=1$ and $\mu_L/\mu_G=50$). k_f is a constant parameter which determine the width of the interface and k_g is a constant parameter which determines the strength of the interfacial tension. E is the weighting factor, $\boldsymbol{c}$ is the particle velocity. H and F are the constant parameters and are defined as:

$$
\begin{aligned}
&E_0=\frac{4}{9},E_1=...=E_4=\frac{1}{9},E_5=...=E_8=\frac{1}{36}\\
&H_0=1,H_1=...=H_8=0,F_0=-\frac{5}{3}\\
&F_i=3E_i\ \ (i=1,2,3,...,8),
\end{aligned}
\tag{7}
$$

And

$$
G_{\alpha\beta}(\phi)=\frac{9}{2}\frac{\partial\phi}{\partial x_\alpha}\frac{\partial\phi}{\partial x_\beta}-\frac{9}{4}\frac{\partial\phi}{\partial x_\gamma}\frac{\partial\phi}{\partial x_\gamma}\delta_{\alpha\beta}
\tag{8}
$$

where subscripts α and β show Cartesian coordination, $\delta_{\alpha\beta}$ is the Kronecker delta.

In Eq. 5 p_0 is thermodynamic pressure which would be defined as:

$$
p_0=\phi T\frac{1}{1-b\phi}-a\phi^2
\tag{9}
$$

where a, b and T are the free parameters to determine maximum and minimum values of ϕ . The following approximations are used to calculate derivatives of Eqs.(5, 6, 8):

$$
\frac{\partial\phi}{\partial x_\alpha}\approx\frac{1}{6\Delta x}\sum_{i=1}^{8}c_{i\alpha}\psi(x+c_i\Delta x)
\tag{10}
$$

$$
\nabla^2\phi\approx\frac{1}{3\Delta x^2}\left[\sum_{i=1}^{8}\phi(x+c_i\Delta x)-8\phi(x)\right]
\tag{11}
$$

The density in interface is determined by maximum and minimum of the order parameter for ϕ_L^* and ϕ_G^* liquid and gas phases through following relation:

$$
\rho=\begin{cases}\rho_g & \phi<\phi_G^*\\ \dfrac{\Delta\rho}{2}\left[\sin\left(\dfrac{\phi-\bar{\phi}^*}{\Delta\phi^*}\pi\right)+1\right]+\rho G, & \phi_G^*\le\phi\le\phi_L^*\\ \rho_l, & \phi>\phi_L^*,\end{cases}
\tag{12}
$$

ρ_G and ρ_L are the density of gas and liquid phase, respectively, $\Delta\rho=\rho_L-\rho_G$, $\Delta\phi^*=\phi_L^*-\phi_G^*$, $\bar{\phi}^*=\left(\phi_L^*+\phi_G^*\right)/2$. The viscosity μ in interface is defined as follows:

$$
\mu=\frac{\rho-\rho_G}{\rho_L-\rho_G}\left(\mu_L-\mu_G\right)+\mu_G
\tag{13}
$$

Where μ_G and μ_L are the viscosity of liquid and gas phase respectively. Surface tension σ is shown by:

$$
\sigma=k_g\int_{-\infty}^{\infty}\left(\frac{\partial\rho}{\partial\xi}\right)^2d\xi
\tag{14}
$$

where ξ represents the coordinate normal to the interface. Since u^* is not divergence free $\left((\nabla.u^*\neq0)\right)$ some corrections are imposed on u^*. Flow velocity u which should satisfy continuity equation $\left(\nabla.u=0\right)$ is obtained as:

$$
Sh\frac{u-u^*}{\Delta t}=-\frac{\nabla p}{\rho}
\tag{15}
$$

$$
\nabla.\left(\frac{\nabla p}{\rho}\right)=Sh\frac{\nabla.u^*}{\Delta t}
\tag{16}
$$

where $Sh=U/c$ is a dimensionless number which is employed by Inamuro[4], p is lattice pressure. The following distribution function is used to calculate pressure:

$$
h_i^{n+1}(x+c_i\Delta x)=h_i^n(x)-\frac{1}{\tau_h}\left[h_i^n(x)-E_iP^n(x)\right]-\frac{1}{3}E_i\frac{\partial u_\alpha^*}{\partial x_\alpha}\Delta x
\tag{17}
$$

where n is the number of iteration and the relaxation time τ_h is defined as:

$$
\tau_h=\frac{1}{\rho}+\frac{1}{2}
\tag{18}
$$

The pressure is attained by:

$$
p=\sum_{i=0}^{8}h_i
\tag{19}
$$

The iteration of Eq. (17) would be continued until $\left|p^{n+1}-p^{n}\right|/\rho<\varepsilon$ is satisfied in the whole domain.

3. Result

3.1. Validation of Two-Phase Solution

Since the most important and sophisticated part of an analysis of two-phase flow is related to dynamic interface between two fluids, first step for the demonstrating accuracy of the flow simulation is checking this issue. Two tests were carried out for this issue. In the first test, deformation of a two dimensional square bubble that has been placed in filled environment of liquid has been shown. According to effects of surface tension between two fluids, the bubble tends to change to steady state with the lowest interface. According to simulation results shown in Fig. 1, bubble shape has changed by passing the time and became like a circle. This issue shows the effects of surface tension, which are important part of two-phase flow analysis, are properly. This test is used as a credit of two-phase solution by Mousavi et al. [19] .

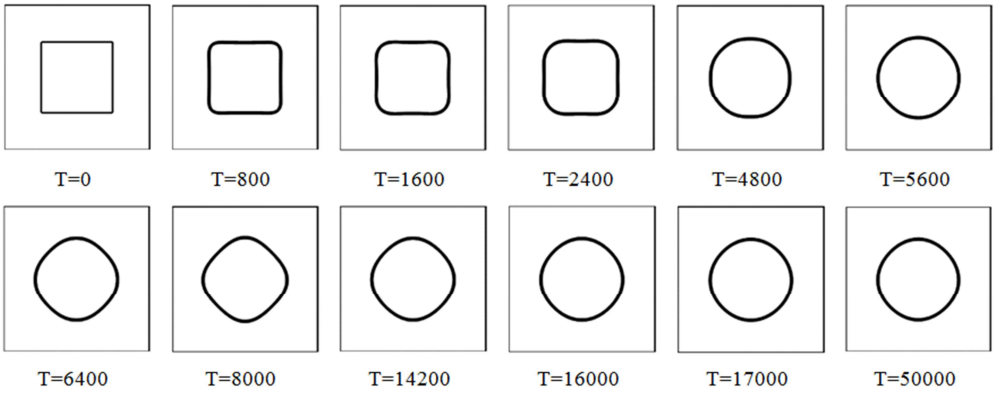

Fig. 1. A square droplet deformation at lattice time steps for density difference 50.

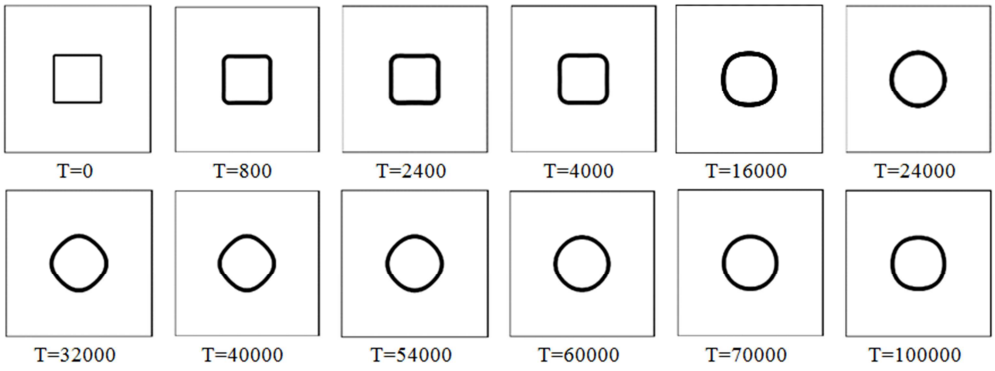

Fig. 2. A square droplet deformation at lattice time steps for density difference 1000.

This test has been done for large density ratio (1000). As Inamuro in [4] mentioned, increasing of density ratio leads to increasing the iteration numbers to achieve desired results. As Fig. 2 shows, deformation occurred in more iterations.

For a static bubble, the velocity must be zero at all points in equilibrium condition. However, in two-phase numerical methods, a spurious nonphysical velocity is created around the bubble near the interface. Indeed today, the numerical methods are improving for decreasing this spurious velocity [20]. Because of this spurious non-physical velocity in numerical methods, weak vortices are created around the droplet and bubble, near interface these velocities have been called parasitic flow. Fig. 3 shows a parasitic flow around a bubble in an equilibrium condition in one of the performed simulations.

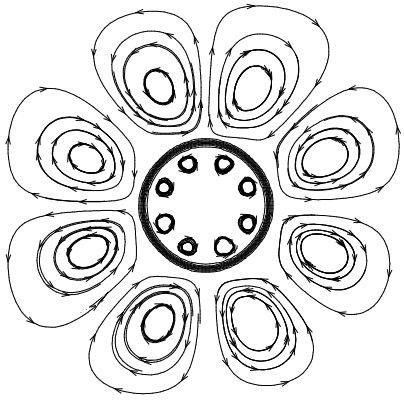

Fig. 3. The parasitic flow around a bubble.

In second test, two circular bubbles with same diameter *L/3* have been located adjacent to each other. In this simulation the distance between two bubbles, density and viscosity are equal to 0/05, 1 and 0.01, respectively. Due to effects of surface tension and Van der Waals forces, these bubbles approach and finally a circular larger bubble is created. The results of this simulation have been shown in Figs. 4-5. This test has been used as a credit of two-phase solution [18, 19].

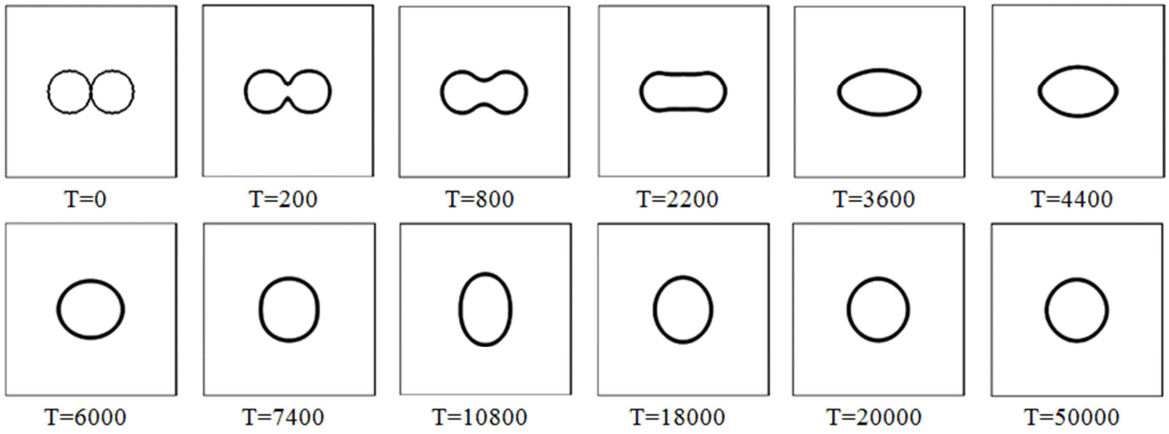

Fig. 4. Coalescence of two bubbles in density ratio 50.

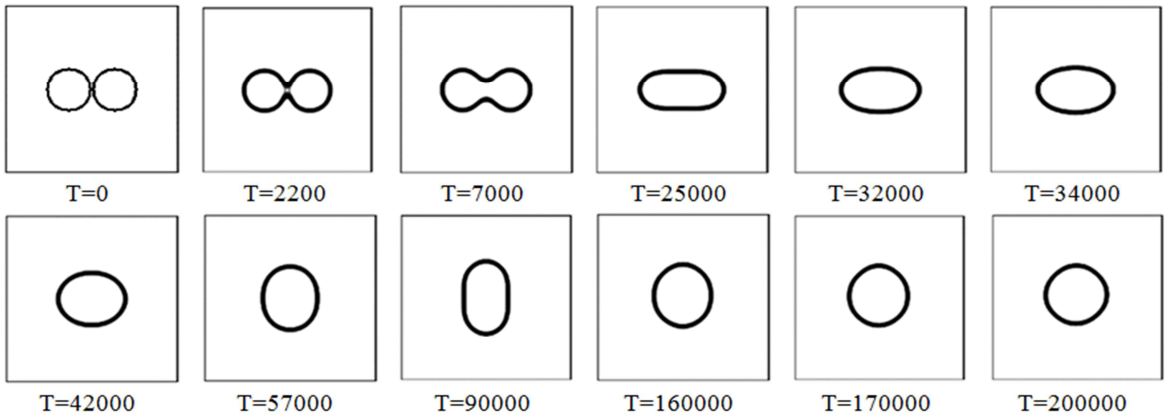

Fig. 5. Coalescence of two bubbles in density ratio 1000.

3.2. Laplace Law

Laplace law represents the correlation between inner P_{in} and outer pressure P_{out} of bubble with interfacial tension σ between two fluids. Based on Laplace law there is formula for a two dimensional bubble [1]:

$$P_{in} - P_{out} = \frac{\sigma}{R} \tag{20}$$

Surface tension during the compressibility and isothermal flows is one of the constant properties of two fluids. Therefore, it can be concluded that a linear relationship exists between the pressure difference between the inside and outside the bubble with the inverse radius in the same conditions without changing its properties. Fig. 6 shows the performed simulation and obtained pressure has been satisfied nicely the Laplace law in Lattice Boltzmann Method. This test has been done as credit of two-phase solution in [1, 3, 18, 19].

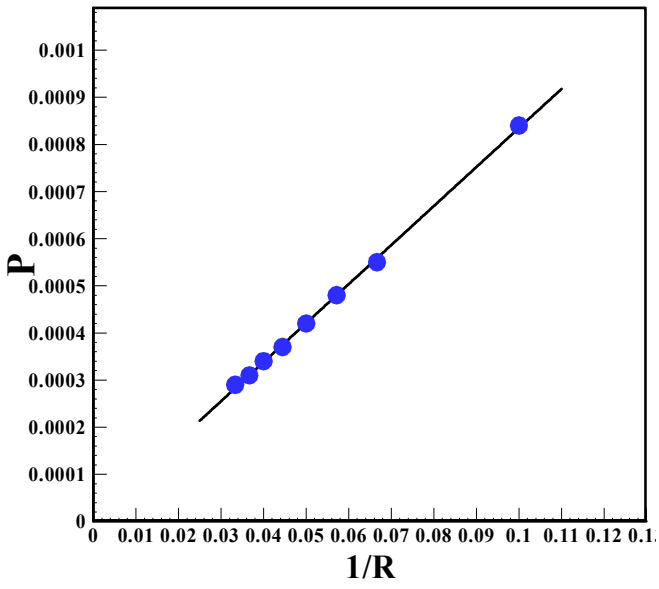

(a)

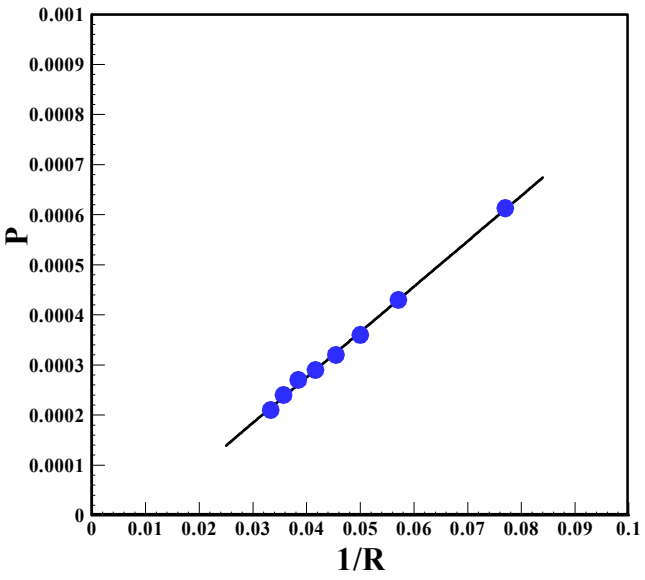

(b)

Fig. 6. Simulation for Laplace law (a) density ratio 50 and (b) density ratio 1000.

3.3. Independence of Mesh

To do this, two different tests have been performed. In the first test, Laplace law has been performed for various grids and note that the related slop is equal to surface tension so the values have been obtained and compared in different grids. In second test, three different grids 200×100, 100×50, 300×150 have been used and the bubble final regimes have been compared. The results of the first test have been shown in Fig. 7 and table 1, due to these results, suggested grid number 100 is for length of the domain, because of the equality of surface tension force in 100×100 and 120×120 grids.

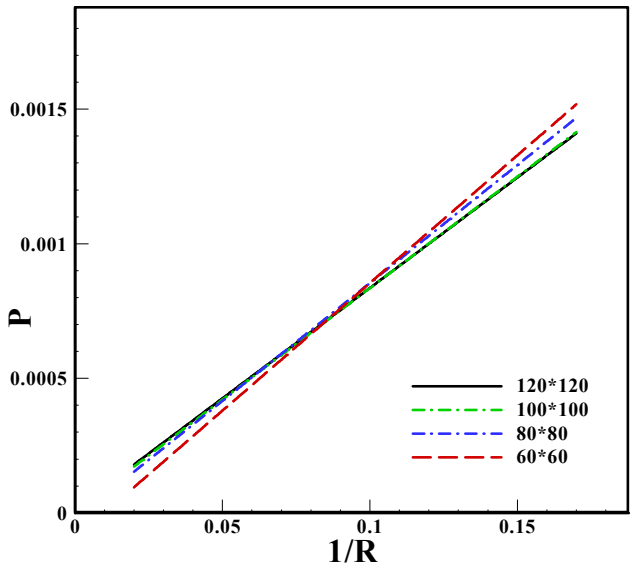

Fig. 7. Laplace law in different grids.

Table 1. The surface tension force in lattice unit In different grids.

Mesh	60×60	80×80	100×100	120×120
Surface tension	0.0094	0.0088	0.0082	0.0081

The results of second test have been shown in table 2; the final shape of the bubble is not true in grid 50×100 by changing of dimensionless numbers in comparison with previous works. However, the final shapes of the bubble and flow regimes in 200×100,300×200 grids are equal. In this paper, 200×100 grid has been used in order to avoid increasing the computational cost.

Table 2. Flow regimes in different dimensionless numbers.

Dimensionless numbers	50×100	100×200	150×300
$E=1, M=0.001$	Spherical	spherical	Spherical
$E=5, M=0.001$	Spherical	ellipsoidal	Ellipsoidal
$E=116, M=266$	Spherical	ellipsoidal cap	ellipsoidal cap
$E=20, M=0.0001$	Ellipsoidal	disc	Disc
$E=42, M=0.001$	ellipsoidal cap	spherical cap	spherical cap
$E=339, M=43$	Skirt	skirt	Skirt

3.4. Rising Bubble

In this section, the bubble motion in a fluid-filled environment has been investigated. The dimensionless numbers of this phenomenon are Morton ($M = g\mu_L(\rho_L - \rho_G)/\rho_L^2\sigma^3$), Etvos ($Eo = g(\rho_L - \rho_G)D^2/\sigma$) and Reynolds numbers ($Re = \rho_L DV/\mu_L$) which V is final velocity of the bubble and D is the initial diameter of the bubble. The opposite boundaries have the periodic boundary conditions. The grid 100×200 has been used. The initial diameter of the bubble has been30-lattice unit.

Behaviour comparison of bubble has been indicated that bubble deformation is a function of Etvos and Morton numbers [4] . According to the terminal shape of bubble which vary in different dimensionless numbers, various patterns of flow in two-phase flow are divided to six major groups are shown in Fig. 8 : 1)spherical, 2)ellipsoidal, 3)ellipsoidal cap, 4)disk, 5)spherical cap, 6)skirt [4] .

The results have been represented in dimensionless time $T = t/t_n$ with $t_n = \sqrt{d/g}$ where t is number of iteration. When the bubble move upward, at first, the bubble starts to move due to density difference with the surrounding fluid leads to buoyancy force. The drag force on the bubble is because of the bubble motion in the fluid and if the bubble does not burst, will reach to the constant velocity and shape. In this mode, buoyancy force is equal to drag force and the bubble continues to move with the constant velocity.

In Fig. 8 in right column, density linear contours with velocity vectors have been drawn for related dimensionless

numbers when the shape of bubble is stable and in left column, movement and shape of the bubble have been shown in different dimensionless times. As seen in Fig. 8, the shape of the bubble is the same for each of the regimes in last dimensionless times due to equivalence between buoyancy and drag forces and stable bubble. As the flow is unstable in Fig. (8.f), the bubble bursts and some of its parts separate after T=5. As seen in Fig. 8, bubble deformation is such as concavity in the bottom of the bubble. In the lower part of the bubble, it should balance itself with its inside pressure, because of the hydraulic pressure, convexity in liquid and concavity inside the bubble has been formed. The larger pressure difference creates the larger vortex around the bubble and as a result, deformation of bubble is more.

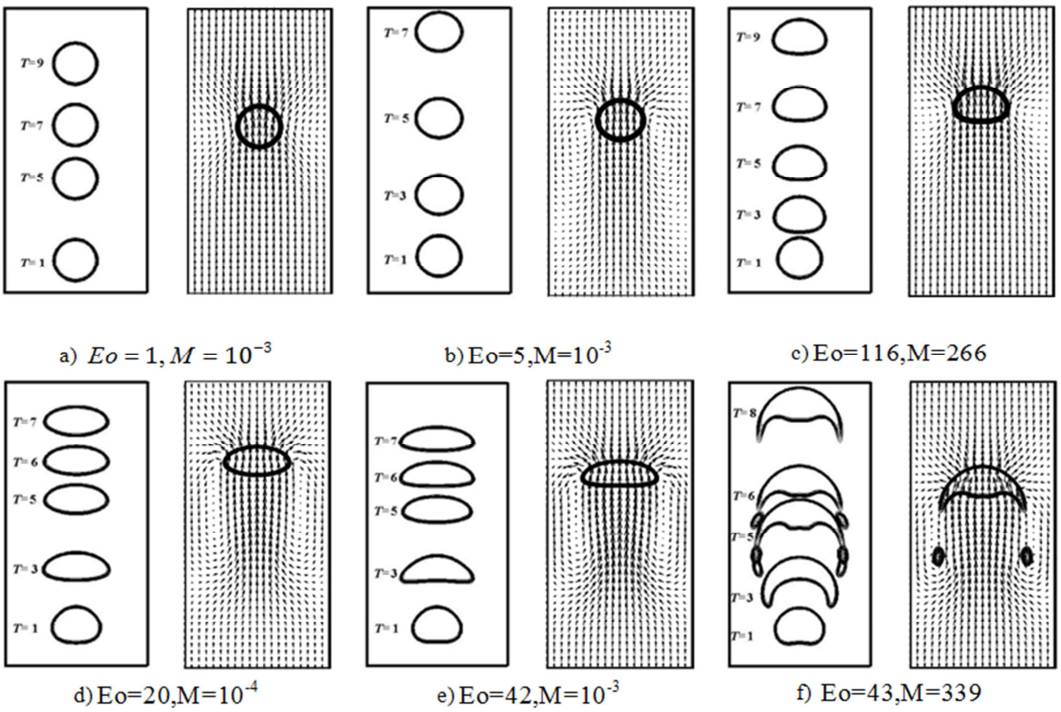

Fig. 8. Different flow regimes in different dimensionless numbers.

In Fig. (8. a) the mentioned vortex area approximately has not been formed so the shape of bubble is stable. From Fig. (8. b) onward the size of this area have been increased so the bubble deformation have been increased. Fig. (8. a) bubble deformation is not large, as is evident from the definition of dimensionless numbers, with the increasing of Etvos number as shown in Figs. (8.a) and (8.b) buoyancy force has been increased and thus deformation of bubble is more. The surface tension decreases by increasing Etvos number, because the surface tension is resistance to deformation, in other hand, increasing of Etvos number causes the increasing of deformation. Moreover increasing of Morton number causes increasing of bubble deformation but have less effect on bubble deformation, because the Morton number relates with the surface tension in power 1/3 as seen on Figs. (8.d) and (8. e).

According to different dimensionless times in Fig. 8, changing dimensionless numbers has showed that required time for passing the length of the channel has been changed and this represents the change in velocity and terminal Reynolds. In Table 3, the terminal Reynolds number values have been calculated

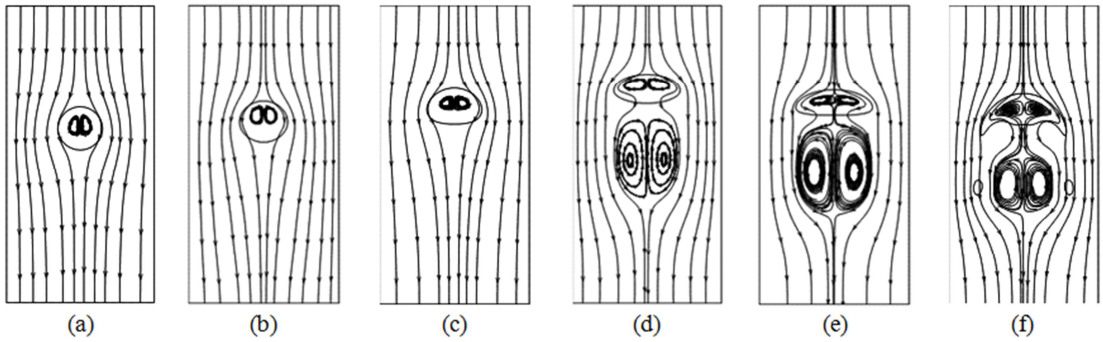

Fig. 9. Streamlines at different dimensionless numbers.

In Fig. 9, streamlines for these bubbles have been plotted. In the first three cases, vortices have been formed only inside the bubble but after Fig. (9.d) vortices have been formed under the bubble that called bubble trail. Bubble trail leads to turbulent flow around the bubble.

In the Fig. 10, the obtained results are in good agreement in compared to Inamuro's three dimensional study [4].

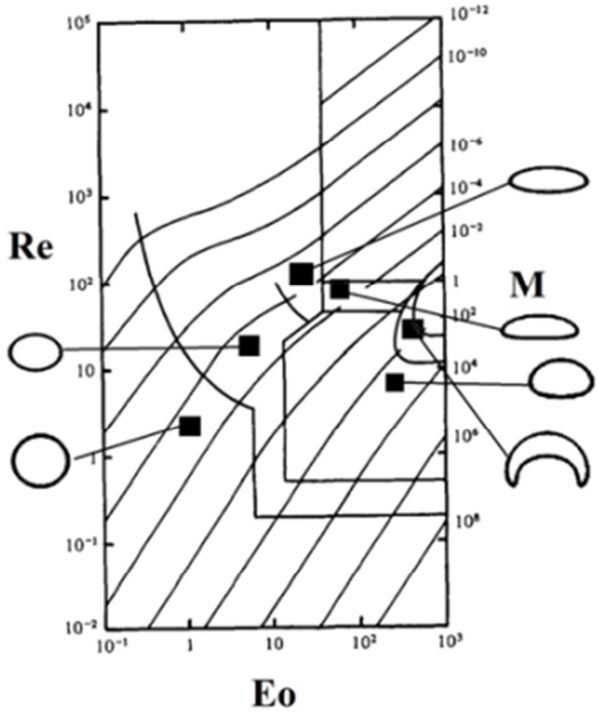

Fig. 10. Comparison of result of this study, ■, and Inamaru's three dimensional study [4].

Table 3. Obtained Re number.

Dimensionless number	The Re of 2D	The Re of 3D	Error of 2D simulation
1) Eo=1,M=10^{-3}	4.62	4.54	%1.76
2) Eo=5,M=10^{-3}	21.95	22.81	%3.77
3) Eo=116,M=266	7.63	7.5	%1.73
4) Eo=20,M=10^{-4}	105.08	109.8	%4.49
5) Eo=42,M=10^{-3}	93.47	100.55	%7.04
6) Eo=43,M=339	34.84	29.45	%18.30

Moreover, this phenomenon has been simulated in three dimensions and the three-dimensional results have been compared with two-dimensional results. Table 3 shows the values obtained for Reynolds number in both cases. Results of 3D have been compared with two-dimensional simulation and error of 2D solution has been calculated. The results show that assumption two-dimensional flow at low terminal Reynolds number have less error than the high Reynolds number and in case of unstable bubble due to high terminal Reynolds number, error of 2D simulation is large. It is established fact now that most phenomena in real world are simulated in 2D such chip devices cooling.

According to the presented results, by comparing Reynolds numbers in f mode, 2D numerical simulation error is large. Therefore, in this case, the bubble is ruptured and in 2D simulation bubble, rupture cannot be modelled.

By comparing Figs. 1-4, it is concluded that in a large density ratio, the same results can be achieved by more iterations. The results are given mainly in density ratio of 50, only an example of density ratio 1000 carried out (Fig. 11); According to tests conducted indicate that this method is efficient and accurate in large density ratio.

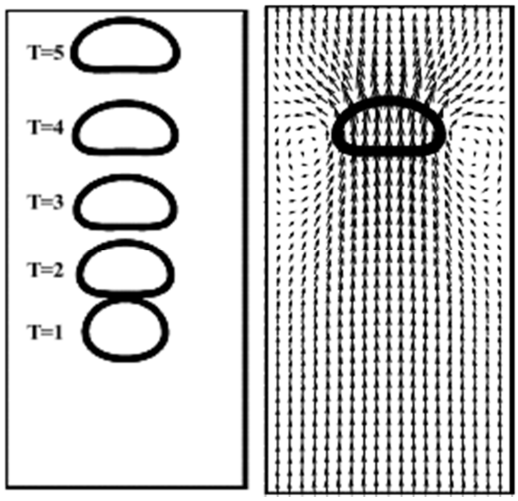

Fig. 11. Rising bubble in density ratio 1000, $E=15, M=1$.

4. Conclusion

In this paper, Inamuro's model has been used to simulate the rising bubble in 3D. The obtained results for the terminal Reynolds number and shape of bubble have been shown very good agreement with the Inamuro's results. Then, because of the high computational cost Inamuro's model, by combining Tanaka and Inamuro's model; Inamuro's model has been used in two-dimensional coordinate system. According to the results of release test of a square in a fluid environment and placed two bubbles together and Laplace law can be used safely this method. By comparing the results, changing in dimensionless numbers have been caused changing in gravity force and surface tension. So different flow regimes occur and Etvos number have a greater impact on the flow regime than the Morton number. By comparing, the results of two-dimensions and three-dimensions have calculated error of 2D simulation. By increasing Re number increases error of two-dimensional solution.

References

[1] A.K. Gunstensen, D.H. Rothman, S. Zaleski, G. Zanetti, *Lattice Boltzmann model of immiscible fluids.* Physical Review A, 1991. 43(8): p. 4320.

[2] X. Shan, H. Chen, *Lattice Boltzmann model for simulating flows with multiple phases and components.* Physical Review E, 1993. 47(3): p. 1815.

[3] M.R. Swift, W. Osborn, J. Yeomans, *Lattice Boltzmann simulation of nonideal fluids.* Physical Review Letters, 1995. 75(5): p. 830.

[4] T. Inamuro, T. Ogata, F. Ogino, *Numerical simulation of bubble flows by the lattice Boltzmann method.* Future Generation Computer Systems, 2004. 20(6): p. 959-964.

[5] T. Inamuro, T. Ogata, S. Tajima, N. Konishi, *A lattice Boltzmann method for incompressible two-phase flows with large density differences.* Journal of Computational Physics, 2004. 198(2): p. 628-644.

[6] T. Inamuro, S. Tajima, F. Ogino, *Lattice Boltzmann simulation of droplet collision dynamics.* International journal of heat and mass transfer, 2004. 47(21): p. 4649-4657.

[7] B. Sakakibara, T. Inamuro, *Lattice Boltzmann simulation of collision dynamics of two unequal-size droplets.* International journal of heat and mass transfer, 2008. 51(11): p. 3207-3216.

[8] T. Inamuro, *Lattice boltzmann methods for viscouse fluid flows and two-phase fluid flows*, in *Computational Fluid Dynamics*. 2008, Springer: India. p. 3-16.

[9] Y.Y. Yan, Y.Q. Zu, *LBM simulation of interfacial behaviour of bubbles flow at low Reynolds number in a square microchannel* in *COMPUTATIONAL METHODS IN MULTIPHASE FLOW V*. 2009. New Forest: WIT Press.

[10] M. Yoshino, Y. Mizutani, *Lattice Boltzmann simulation of liquid–gas flows through solid bodies in a square duct.* Mathematics and computers in simulation, 2006. 72(2): p. 264-269.

[11] Y. Yan, Y. Zu, *A lattice Boltzmann method for incompressible two-phase flows on partial wetting surface with large density ratio.* Journal of Computational Physics, 2007. 227(1): p. 763-775.

[12] Y.Y. Yan, Y.Q. Zu, *Numerical modelling of bubble coalescence and droplet separation*, in *COMPUTATIONAL METHODS IN MULTIPHASE FLOW IV*. 2007, WIT Press: Bologna, Italy. p. 227-237.

[13] Y. Tanaka, Y. Washio, M. Yoshino, T. Hirata, *Numerical simulation of dynamic behavior of droplet on solid surface by the two-phase lattice Boltzmann method.* Computers & Fluids, 2011. 40(1): p. 68-78.

[14] Y. Tanaka, M. Yoshino, T. Hirata, *Lattice Boltzmann simulation of nucleate pool boiling in saturated liquid.* Communications in Computational Physics, 2011. 5.

[15] T. Lee, *Effects of incompressibility on the elimination of parasitic currents in the lattice Boltzmann equation method for binary fluids.* Computers & Mathematics with Applications, 2009. 58(5): p. 987-994.

[16] T. Lee and C.-L. Lin, *A stable discretization of the lattice Boltzmann equation for simulation of incompressible two-phase flows at high density ratio.* Journal of Computational Physics, 2005. 206(1): p. 16-47.

[17] T. Lee and L. Liu, *Lattice Boltzmann simulations of micron-scale drop impact on dry surfaces.* Journal of Computational Physics, 2010. 229(20): p. 8045-8063.

[18] H. Zheng, C. Shu and Y.-T. Chew, *A lattice Boltzmann model for multiphase flows with large density ratio.* Journal of Computational Physics, 2006. 218(1): p. 353-371.

[19] S. E. Mousavi Tilehboni, K. Sedighi, M. Farhadi, E. Fttahi, *Lattice Boltzmann Simulation of Deformation and Breakup of a Droplet under Gravity Force Using Interparticle Potential Model.* International Journal of Engineering-Transactions A: Basics, 2013. 26(7): p. 781.

[20] T. Seta and K. Okui, *Effects of truncation error of derivative approximation for two-phase lattice Boltzmann method.* Journal of Fluid Science and Technology, 2007. 2(1): p. 139-151.